Journal of Solid State Chemistry **161,** 307–311 (2001)
doi:10.1006/jssc.2001.9316, available online at http://www.idealibrary.com on IDEAL®

# Synthesis and Crystal Structure of $C_5H_{12}NPO_4H_2$

K. Kaabi, C. Ben Nasr, and M. Rzaigui

*Laboratoire de Chimie des Matériaux, Faculté des Sciences de Bizerte, 7021 Zarzouna, Tunisia*

Received May 29, 2001; in revised form July 6, 2001; accepted July 16, 2001

**Synthesis and crystal structure are described for a new noncento-symmetric organic-cation monophosphate, $C_5H_{10}NH_2 \cdot H_2PO_4$. This compound is triclinic P1 with the following unit-cell parameters: $a = 6.2397(6)$, $b = 8.4191(7)$, $c = 8.8523(2)$ Å, $\alpha = 112.485(4)$, $\beta = 89.992(4)$, $\gamma = 90.104(7)°$, $V = 429.37(5)$ Å$^3$, $Z = 2$, and $D_x = 0.709\ \mathrm{g\,cm^{-3}}$. Crystal structure was solved with a final $R$ value of 0.03 for 2347 independent reflections. The $H_2PO_4$ groups form, via strong hydrogen bonds, corrugated infinite chains $(H_2PO_4)_n^{n-}$ spreading along the a direction. Between these chains coexist two crystallographically independent organic groups, which connect the chains with hydrogen bonds.** © 2001 Academic Press

***Key Words:*** **crystallization; optical material; X-ray diffraction; crystal structure; hydrogen bond; IR spectroscopy; TG-DTA; MAS-NMR.**

## I. INTRODUCTION

A new class of noncentrosymmetric crystals for quadratic nonlinear optic has recently been developed through a crystal engineering route, which combines the high cohesion of inorganic host matrices with the enhanced polarizability of organic guest chromophores (1). Better performance of optical signal-processing devices should be linked to such new materials (2). The design of organic–inorganic polar crystals for quadratic nonlinear optical applications is derived from and supported by two main observations:

(i) the organic molecules containing Π-bonds asymmetrized by electron donor-acceptor groups are highly polarizable entities in which transparency could be controlled.

(ii) The ionic inorganic host matrices may increase the packing cohesion, shift the transparency of crystals toward blue wavelengths, and induce noncentrosymmetry.

Within a systematic investigation of new materials resulting from the association of organic chromophores with inorganic species we report here the synthesis, crystal structure, and some characteristic properties of a new compound: (pipyridinium) dihydrogenophosphate, $C_5H_{12}PO_4H_2$ including the amine, a chromophore which could be efficient in the blue-u.v. wavelength region. This compound could exhibit a richness of interesting physical properties such as ferroelectricity and nonlinear optic phenomena like second harmonic generation.

## II. EXPERIMENTAL

### II.1. Chemical Preparation

The title compound $C_5H_{10}NH_2.H_2PO_4$ was prepared according to the chemical reaction

$$H_3PO_4 + C_5H_{11}N \rightarrow C_5H_{10}NH_2.H_2PO_4$$

by adding drop wise concentrated orthophosphoric acid to an aqueous solution of pipyridine. The obtained solution was then slowly evaporated at room temperature until $C_5H_{10}NH_2.H_2PO_4$ prisms were formed. The crystals are sparingly soluble in water and stable for months in normal conditions of temperature and humidity.

### II.2. Technical Investigation

The intensity data collection was performed with a MACH3 Enraf Nonius diffractometer. The strategy used for the structure determination and its final results are gathered in Table 1.

Thermal analysis was performed using the Multimodule 92 Setaram analyzer operating from room temperature up to 420°C at an average heating rate of 5°/min.

IR spectra were recorded in the 4000–200 cm$^{-1}$ range with a Spectrum 1000 Perkin–Elmer spectrophotometer using samples dispersed in spectroscopically pure KBr pellets.

Proton-decoupled $^{31}$P MAS NMR spectra were recorded with Bruker DSX-300 solid-state high-resolution spectrometer operating at 121.495 MHz (magnetic field 7.05 T). Pulses (90°) of 5 μs duration were employed with a delay of 5 s between pulses in all experiments. A cylindrical zirconia rotor, adapted to a CP/MAS Doty sonde, was used and spinning rates of 2 and 3.5 KHz were employed. All the spectra were recorded at room temperature. The chemical shift values are given with respect to 85% $H_3PO_4$.

0022-4596/01 $35.00

**TABLE 1**

**Crystal Data, Experimental Parameters Used for the Intensity Data Collection, Strategy, and Final Results of the Structure Determination**

| | |
|---|---|
| I. Crystal data | |
| Formula: $C_5H_{10}NH_2.H_2PO_4$. | $F$w = 183.09 |
| Crystal system: triclinic | Space group $P1$ |
| $a = 6.2397(6)$, $b = 8.4191(7)$, $c = 8.8523(2)$ Å | $Z = 2$ |
| $\alpha = 112.485(4)$, $\beta = 89.992(4)$, $\gamma = 90.104(7)^\circ$ | $V = 429.37(5)$ Å$^3$ |
| Refinement of unit-cell parameters with: 25 reflections | $(10^\circ < \theta < 12^\circ)$ |
| $\rho_{cal.} = 0.709\ g\,cm^{-3}$ | $F(000) = 194$ |
| Crystal size: $0.40 \times 0.25 \times 0.20\,mm^3$ | Morphology: prism |
| Linear absorption factor: $\mu(MoK_\alpha) = 0.185\,mm^{-1}$ | |
| II. Intensity measurements | |
| Diffractometer: Enraf–Nonius MACH3, (292.2 K) | Wavelength: Mo$K_\alpha$ (0.7107 Å) |
| Theta range: 3–30° | Scan mode: $\omega/2\theta$ |
| Measurement area: $\pm h$, $\pm k$, $l$ | $h_{max.} = 8$, $k_{max.} = 11$, $l_{max.} = 12$ |
| Number of scanned reflections: 2499 | Number of independent reflections: 2347 |
| Two intensity and orientation control reflections: $\bar{3}\ \bar{2}\ 3$ and $\bar{1}\ \bar{3}\ \bar{2}$, no variation | |
| III. Structure determination | |
| Lorentz and polarization corrections | No absorption correction |
| Determination: a direct method SIR92 (3) | Program used: TeXsan (4) |
| Thermal displacement parameters: isotropic for H atoms, anisotropic for non-H atoms. | |
| Unique reflections included: 2347 with $I > 3\,\sigma(I)$ | Refined parameters: 308 |
| Agreement factors $R$: 0.035, $R$w: 0.040 | Largest shift/error: 0.08 |
| Residual Fourier density: $-0.54 < \rho < 0.26\ e\,Å^{-3}$ | Esd: 0.84 |
| Drawings made with MolView (5) | |

## III. RESULTS AND DISCUSSION

### III.1. Crystallographic Study

The structural determination shows that the title compound crystallizes in the triclinic system with $P1$ space group, which is confirmed by a positive second harmonic generation powder test observed on a sample illuminated by YAG $Nd^{3+}$ laser radiation at 1.06 μm. The final atomic coordinates of all nonhydrogen atoms and their $B_{eq}$ are given in Table 2. Those of hydrogen atoms were also determined but are not given, in order to shorten the table.

The atomic arrangement of $C_5H_{12}NPO_4H_2$ is projected in the $(a, c)$ plane (Fig. 1). This projection shows that the $(H_2PO_4)^-$ dihydrogenophosphate groups are interconnected via hydrogen bonds to form corrugated infinite chains which develop parallel to the **a** direction in (001) planes. Between these chains we find the organic entities which are connected to them with hydrogen bonds. Inside such a chain, there are two crystallographically independent $PO_4$ tetrahedra. Their main geometrical features are reported in Table 3. In this chain organization of $(H_2PO_4)^-$ entity, it is noteworthy that the O … O distances involved in hydrogen bonds (2.574(2) to 2.634(4) Å) are of the same magnitude as the O–O edge in the $PO_4$ tetrahedra (2.450(2) to 2.546(2) Å), this should allow us to consider the $[H_2PO_4]_n^{n-}$ subnetwork as a system of polyanions. This result agrees with the $C_3H_8NO_2^+H_2PO_4^-$ data observed elsewhere (6).

The detailed geometry of $(H_2PO_4)^-$ anions shows that the P–O bonds are significantly shorter (1.494(1) to 1.515(1) Å) than the P–OH bonds (1.564(1) to 1.575(1) Å), which agrees with the previous data relative to the protonated oxoanions (7).

Examination of the main geometrical features (Table 3) of the two independent $PO_4$ tetrahedra shows three different types of O–P–O angles. The HO–P–OH, angles which correspond to the largest P–O bonds, are close to 103°. The HO–P–O angles have an average value expected of a regular tetrahedron. The O–P–O angles of $H_2PO_4$, corresponding to the shortest P–O distances, have values close to 115°. This is probably induced by the mutual repulsion of the

**TABLE 2**

**Final Atomic Coordinates and $B_{eq}$ for the Nonhydrogen Atoms**

| Atoms | $x(\sigma)$ | $y(\sigma)$ | $Z(\sigma)$ | $B_{eq.}$ (Å$^2$) |
|---|---|---|---|---|
| P(1) | 0.0000 | 0.0000 | 0.0000 | 1.956(5) |
| P(2) | − 0.50005(7) | − 0.36833(5) | − 0.12300(5) | 1.957(5) |
| O(11) | − 0.4342(3) | − 0.5238(2) | − 0.0917(2) | 3.31(2) |
| O(12) | − 0.3564(3) | − 0.3444(2) | − 0.2591(2) | 3.24(2) |
| O(13) | − 0.0027(2) | − 0.1664(2) | − 0.1495(2) | 2.54(2) |
| O(14) | − 0.5030(2) | − 0.2022(2) | 0.0257(1) | 2.51(2) |
| O(21) | − 0.7252(2) | − 0.4099(2) | − 0.2069(2) | 2.79(2) |
| O(22) | − 0.2257(2) | 0.0409(2) | 0.0832(2) | 2.76(2) |
| O(23) | 0.1441(3) | − 0.0241(2) | 0.1356(2) | 3.23(2) |
| O(24) | 0.0658(3) | 0.1558(2) | − 0.0313(2) | 3.34(2) |
| N(1) | − 0.1521(3) | − 0.5425(2) | 0.1345(2) | 2.46(2) |
| N(2) | − 0.6519(3) | 0.1742(2) | − 0.2580(2) | 2.43(2) |
| C(1) | 0.1932(4) | − 0.4137(3) | 0.2493(3) | 3.98(4) |
| C(2) | − 0.4967(4) | 0.0345(3) | − 0.2727(3) | 3.42(3) |
| C(3) | 0.0035(4) | − 0.4035(3) | 0.1483(3) | 3.38(3) |
| C(4) | − 0.3060(4) | 0.0452(4) | − 0.3728(3) | 4.01(4) |
| C(5) | − 0.2292(3) | − 0.5346(3) | 0.2963(2) | 3.08(3) |
| C(6) | − 0.7291(3) | 0.1665(3) | − 0.4200(2) | 3.07(3) |
| C(7) | − 0.5407(4) | 0.1801(3) | − 0.5216(2) | 3.50(3) |
| C(8) | − 0.3737(4) | 0.0397(3) | − 0.5401(3) | 4.01(4) |
| C(9) | − 0.0404(4) | − 0.5477(3) | 0.3985(2) | 3.52(3) |
| C(10) | 0.1255(4) | − 0.4080(4) | 0.4166(3) | 4.09(4) |

*Note.* Estimated standard deviations are given in parentheses.

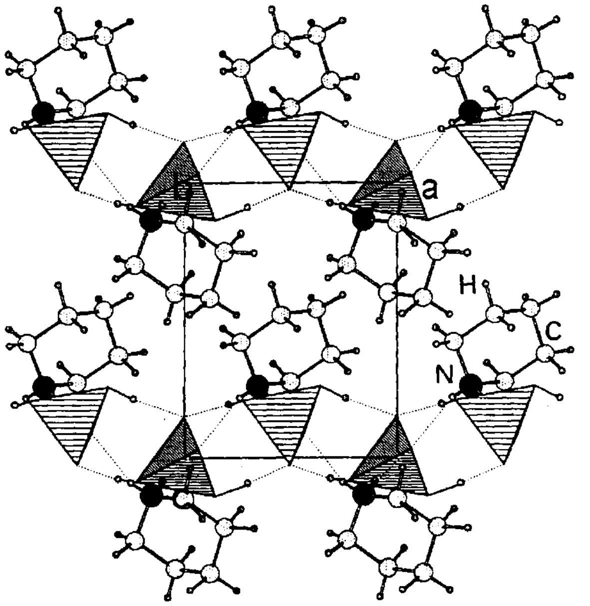

**FIG. 1.** The atomic arrangement of $C_5H_{10}NH_2 \cdot H_2PO_4$ in projection along the *b* axis. The $PO_4$ groups are given in the tetrahedral representation. Hydrogen bonds are denoted by dotted lines.

nonbridging oxygen atoms. Nevertheless, the calculated average values of the distortion indices (8) corresponding to the different angles and distances in the independent $PO_4$ tetrahedra are:

For the $P(1)O_4$ tetrahedra, ID(PO) = 0.021 ID(OPO) = 0.029 ID(OO) = 0.014

### TABLE 3
### Main Interatomic Distances (Å) and Bond Angles (°) in the $PO_4$ Tetrahedra of $C_5H_{10}NH_2 \cdot H_2PO_4$

$P(1)O_4$ Tetrahedron

| P(1) | O(11) | O(12) | O(13) | O(14) |
|---|---|---|---|---|
| O(11) | 1.515(1) | 2.546(2) | 2.515(2) | 2.540(2) |
| O(12) | 111.5(6) | 1.566(1) | 2.457(2) | 2.452(2) |
| O(13) | 109.1(6) | 103.0(7) | 1.574(1) | 2.535(2) |
| O(14) | 115.0(7) | 106.4(7) | 111.3(8) | 1.497(1) |

| | |
|---|---|
| O(12)–H(1) = 0.98(3) | H(1)–O(12)–P(1) = 117(2) |
| O(13)–H(2) = 1.12(4) | H(2)–O(13)–P(1) = 115(2) |

$P(2)O_4$ Tetrahedron

| P(2) | O(21) | O(22) | O(23) | O(24) |
|---|---|---|---|---|
| O(21) | 1.494(1) | 2.532(1) | 2.537(1) | 2.451(2) |
| O(22) | 111.2(8) | 1.575(1) | 2.514(2) | 2.450(2) |
| O(23) | 115.2(7) | 109.2(7) | 1.510(1) | 2.541(2) |
| O(24) | 106.5(7) | 102.6(8) | 111.5(6) | 1.564(1) |

| | |
|---|---|
| O(22)–H(3) = 0.85(3) | H(3)–O(22)–P(2) = 105(2) |
| O(24)–H(4) = 0.74(3) | H(4)–O(24)–P(2) = 112(2) |

*Note.* Estimated standard deviations are given in parentheses.

### TABLE 4
### Main Interatomic Distances (Å) and Bond Angles (°) in the $C_5H_{11}N$ Groups

| Bonds | Angles |
|---|---|
| $C_5H_{12}N(1)$ group | |
| N(1)–C(1) = 1.487(2) | C(1)–N(1)–C(5) = 112.7(2) |
| C(1)–C(2) = 1.505(3) | C(2)–C(1)–N(1) = 109.9(2) |
| C(2)–C(3) = 1.523(3) | C(3)–C(2)–C(1) = 111.8(2) |
| C(3)–C(4) = 1.527(3) | C(4)–C(3)–C(2) = 110.4(2) |
| C(4)–C(5) = 1.515(3) | C(5)–C(4)–C(3) = 111.2(2) |
| C(5)–N(1) = 1.489(2) | N(1)–C(5)–C(4) = 109.7(1) |
| $C_5H_{12}N(2)$ group | |
| N(2)–C(6) = 1.490(2) | C(6)–N(2)–C(10) = 112.6(1) |
| C(6)–C(7) = 1.506(3) | C(7)–C(6)–N(2) = 110.1(2) |
| C(7)–C(8) = 1.524(3) | C(8)–C(7)–C(6) = 111.5(2) |
| C(8)–C(9) = 1.537(3) | C(9)–C(8)–C(7) = 110.4(3) |
| C(9)–C(10) = 1.511(3) | C(10)–C(9)–C(8) = 111.2(2) |
| C(10)–N(2) = 1.491(2) | N(2)–C(10)–C(9) = 109.6(2) |

*Note.* Estimated standard deviations are given in parentheses.

For the $P(2)O_4$ tetrahedra, ID(PO) = 0.022 ID(OPO) = 0.030 ID(OO) = 0.014

These values show an above distortion of the P–O distance compared to the O–O distances. The $PO_4$ tetrahedron is thus described by regular oxygen-atom arrangement with the phosphorus atom shifted from the gravity center of $PO_4$.

In this atomic arrangement, there exist two independent organic cations [$C_5H_{12}N(1)^+$, $C_5H_{12}N(2)^+$]. Table 4 reports values of all bond distances and angles in these groups. The $NH_2$ groups are anchored onto both adjacent anionic ribbons by N–H…O hydrogen bonds to form a stable tridimensional network. The main geometrical features of the hydrogen bonds are described in Table 5.

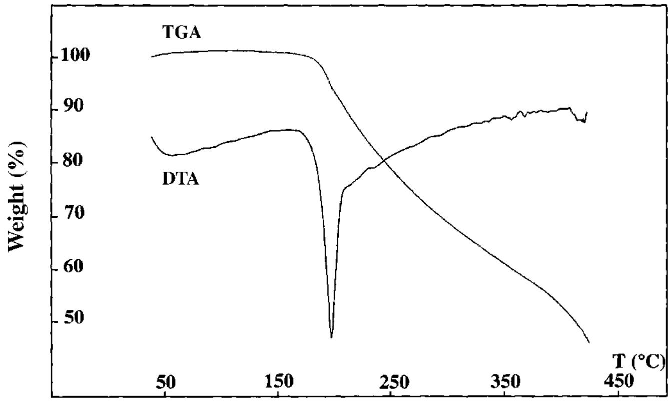

**FIG. 2.** DTA and TGA curves of $C_5H_{10}NH_2 \cdot H_2PO_4$ at rising temperature.

**TABLE 5**
**Hydrogen-Bond Scheme in $C_5H_{10}NH_2 \cdot H_2PO_4$**

| N(O)–H...O | N(O)–H | H...O | N(O)...O | N(O)–H...O |
|---|---|---|---|---|
| O(12)–H(2)...O(23) | 0.89(3) | 1.71(3) | 2.574(2) | 164(3) |
| O(13)–H(1)...O(23) | 1.12(4) | 1.52(4) | 2.634(4) | 171(3) |
| O(22)–H(3)...O(11) | 0.85(4) | 1.82(4) | 2.633(2) | 160(4) |
| O(24)–H(4)...O(11) | 0.74(3) | 1.86(3) | 2.582(2) | 165(3) |
| N(1)–H(1N1)...O(21) | 0.78(3) | 1.97(3) | 2.716(2) | 158(3) |
| N(1)–H(2N1)...O(14) | 0.85(5) | 1.92(3) | 2.758(2) | 169(3) |
| N(2)–H(1N2)...O(21) | 0.90(3) | 1.86(5) | 2.756(2) | 175(3) |
| N(2)–N(2N2)...O(14) | 0.70(3) | 2.05(3) | 2.718(2) | 161(3) |

*Note.* Estimated standard deviations are given in parentheses.

### *III.2. Thermal Analysis*

The two curves corresponding to DTA and TGA analysis in open air are given in Fig. 2. The DTA curve exhibits an endotherm at 200°C, attributed to the further malting and beginning of degradation of the compound. Since this endotherm corresponds to the combination of two phenomena, the TGA curve shows a continuous weight loss of 46.99% between 237 and 420°C. The analyzed phosphate is stable until it is expounded by the presence of strong hydrogen bonds in the anhydrous compound determined by X-ray diffraction study.

### *III.3. IR Absorption Spectroscopy*

The infrared absorption spectrum is reported in Fig. 3. It exhibits:

bands with frequencies in the 3450–2300 cm$^{-1}$ range, attributed to the stretching modes of organic and hydroxyl groups,

bending vibration bands between 1650 and 1200 cm$^{-1}$ corresponding to the organic group, and

various valancy and bending vibration bands whose number and positions, between 1200 and 300 cm$^{-1}$, are characteristic of a monophosphate (9).

The PO$_4$ tetrahedra give two stretching vibrations $\nu_s$ and $\nu_{as}$, respectively, symmetric and asymmetric. These vibration bands are observed about 1000–850 cm$^{-1}$ and 500–300 cm$^{-1}$. The tetrahedra PO$_4$ also presents two

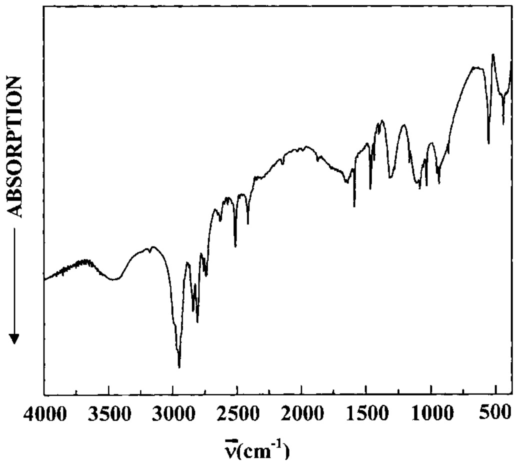

**FIG. 3.** IR spectrum of $C_5H_{10}NH_2 \cdot H_2PO_4$ in KBr.

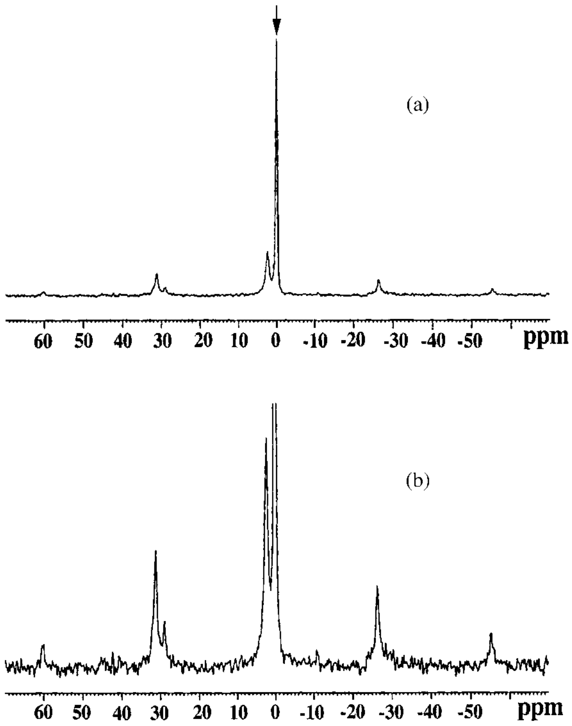

**FIG. 4.** (a) $^{31}P$ MAS NMR spectra of the crystalline monophosphate $C_5H_{10}NH_2 \cdot H_2PO_4$. Signals are marked by an arrow; sidebands are left unsuppressed; spinning rate = 3.5 KHz. (b) The same spectra with an amplitude 4 times more important.

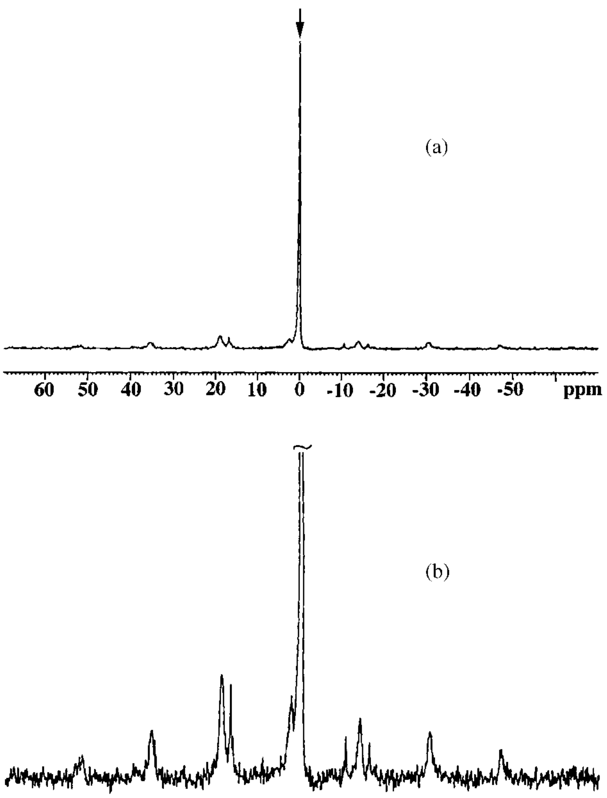

**FIG. 5.** (a) $^{31}P$ MAS NMR spectra of the crystalline monophosphate $C_5H_{10}NH_2 \cdot H_2PO_4$. Signals are marked by an arrow; sidebands are left unsuppressed; spinning rate = 2 KHz. (b) The same spectra with an amplitude 8 times more important.

bending vibration bands $\nu_s$ and $\nu_{as}$, which are observed between 1200–1000 cm$^{-1}$ and 650–500 cm$^{-1}$, respectively.

### *III.4. NMR Spectroscopy*

The $^{31}P$ NMR chemical shifts of monovalent cation monophosphates are generally positive (10–16). Proton-decoupled $^{31}P$ MAS NMR spectra of polycrystalline $C_5H_{12}NPO_4H_2$ are presented in Figs. 4 and 5. These figures show two resonance peaks. The respective chemical shifts 0.15 and 0.96 ppm were recorded with respect to 85% $H_3PO_4$ (positive chemical shifts are toward lower fields in spectra). The number of signals are related to the number of crystallographically distinguishable phosphorous sites. The distance of spinning sidebands from isotropical position (marked by arrow in spectra) is a multiple of the rotor spinning rate. Thus, for the spectrum registered with a frequency of 3.5 KHz, the spinning sidebands appear at $\pm$ 3.5 KHz (3500/121.495 = 28.8 ppm), then at $\pm 2 \times 3.5$ KHz = $\pm$ 7.0 KHz (Fig. 4). Obviously, for the spectrum registered with a spinning rate of 2.0 KHz, the spinning sidebands are nearer because we find them at the distance of $\pm$ 2 KHz (Fig. 5). These spectra also show that only the phosphorous site at 2.96 ppm has a pronounced spinning sideband intensity compared with the central position (isotropical position). This points out that the chemical shift anisotropy is strongly marked for the phosphorous site at 2.96 ppm. Therefore, the electonical distribution around this phosphorous site is more asymmetrical than the site at 0.15.

To compare the relative percentages of these sites, we necessarily must add the intensities of the isotropical signals and their respective spinning sidebands. Figures 4 and 5 show that the intensity sum of the phosphorous site at 2.96 is approximately close to that at 0.15. The comparable relative intensities of the two phosphorous sites obtained in this study agrees therefore with the crystallographical results.

## REFERENCES

1. R. Masse, M. Bagieu-Beucher, J. Pecault, J. P. Levy, and J. Zyss, *Nonlinear Opt.* **5**, 413 (1993).
2. J. Zyss, in J. L. Brédas, and R. R Chance (Eds.), *in* "Conjugated Polymeric Materials: Opportunities in Electronics and Molecular Electronics," p. 545. Kluwer, Dordrecht, 1990.
3. A. Altomare, G. Cascarano, C. Giacovazzo, and A. Guagliardi, *J. Appl. Crystallogr.* **26**, 343 (1993), doi: 10.1107/S0021889892010331.
4. "TeXsan for Windows," Version 1.03, Molecular Structure Corporation, single Crystal Structure Analysis Software, Version 1.03, MSC, 3200 Research Forest Drive, The Woodlands, TX, 1997.
5. J. M. Cense, *in* "Modelar Graphics for the Macintosh (MolView) in Modelling of Molecular Structure and Properties," p. 763. Elsevier, Amsterdam, 1990.
6. M. T. Averbutch-Pouchot, A. Durif, and C. Guitels, *Acta Crystallogr. Sect. C* **44**, 1968 (1988), doi: 10.1107/S0108270187008539.
7. G. Ferraris and G. Ivaldi, *Acta Crystallogr. Sect. B* **40**, 1 (1984), doi: 10.1107/S0108768184001671.
8. W. Baur, *Acta Crystallogr. Sect. B* **30**, 1195 (1974), doi: 10.1107/S0567740874004560.
9. S. Kamoun, M. Kamoun, A. Daoud, and F. Romain, *Spectrochim. Acta, A* **47**, 1051 (1991).
10. A. R. Grimmer and U. Haubenerisser, *Chem. Phys. Lett.* **99**, 487 (1983).
11. D. Müller, E. Jahn, G. Ladwing, and U. Haubenerisser, *Chem. Phys. Lett.* **109**, 332 (1984).
12. S. Prabhakar, K. J. Rao, and C. N. R. Rao, *Chem. Phys. Lett.* **139**, 96 (1987).
13. A. K. Cheetham, N. J. Clayden, C. M. Dobson, and R. J. B. Jakeman, *J. Chem. Soc. Chem. Commun.* 195 (1986).
14. P. Hartmann, J. Vogel, and B. Schnabel, *J. Magn. Reson.* **111**, 110 (1994).
15. L. Mudrakovskii, V. P. Shmochkova, N. S. Kotsarenko, and V. M. Mastikhin, *Phys. Chem. Solids* **47**, 335 (1986).
16. G. L. Turner, K. A. Smith, R. J. Kirkpatrick, and E. Oldfield, *J. Magn. Reson.* **70**, 408 (1986).